JOURNAL OF DEGRADED AND MINING LANDS MANAGEMENT
Volume 9, Number 1 (October 2021):3115-3127, doi:10.15243/jdmlm.2021.091.3115
ISSN: 2339-076X (p); 2502-2458 (e), www.jdmlm.ub.ac.id

Research Article

Assessment of organic carbon contamination in the unsaturated zone: a case of Yogyakarta City, Indonesia

Heru Hendrayana[1*], Doni Prakasa Eka Putra[1], Yosua Priambodo[2]

[1] Department of Geological Engineering, Universitas Gadjah Mada, Jl. Grafika Bulaksumur, Yogyakarta 55284, Indonesia
[2] Groundwater Working Group, Faculty Engineering, Universitas Gadjah Mada, Jl. Grafika Bulaksumur, Yogyakarta 55284, Indonesia

[*]corresponding author: heruhendrayana20@gmail.com

Article history:
Received 22 June 2021
Accepted 3 August 2021
Published 1 October 2021

Keywords:
groundwater
contamination
total organic carbon
unsaturated zone

Abstract

In 1997, groundwater pollution was caused by a diesel leak at the Yogyakarta City Railway Station. People in the south of the railway station discovered the presence of diesel in dug wells in 2001. The existing diesel is still found in dug wells even though the pollutant source had been removed. The current source of pollution comes from diesel residues trapped in the unsaturated zone. Understanding the distribution and concentration of diesel in the unsaturated zone is the goal of this study. In this study, diesel concentration was measured based on Total Organic Carbon (TOC) levels. The research was conducted through shallow core and deep core drillings. Shallow core drilling was done at 14 points with a depth of 50 cm, and deep core drilling was done at nine drilling points with a depth of 15-17 m. 14 shallow core drilling samples were taken from a depth of 30 and 50 cm and nine deep core drilling samples were taken from a depth of 4-5 m and 10-11 m. The lithology logs in both drills were tested for diesel odour and TOC levels using the Soli TOC tool. Based on the test results, the smell of diesel was found at a depth of 10 to 15 m. TOC levels in the unsaturated zone ranged from 340 to 90,870 mg/L. TOC levels >30,000 mg/L were dominant at shallow depths even though they did not smell like diesel. At a location close to the source of the diesel tank leak at a depth of 4-5 m, the measured TOC level was 30,100 mg/L. The results showed that there were zones of high TOC levels associated with diesel odour layers. The zones existed because of the infiltration and percolation processes that had carried surface water and diesel pollutants and eventually moved horizontally following groundwater flow.

To cite this article: Hendrayana, H., Putra, D.P.E. and Priambodo, Y. 2021. Assessment of organic carbon contamination in the unsaturated zone: a case of Yogyakarta City, Indonesia. Journal of Degraded and Mining Lands Management 9(1):3115-3127, doi:10.15243/jdmlm.2021.091.3115.

Introduction

Pollution is the leading cause of deteriorating groundwater quality, especially in urban areas. Pollution is generally caused by human activities, including the use of hydrocarbon diesel (Bedient et al., 1999). The movement of organic chemical pollutants is related to the flow of water that passes through the unsaturated zone. The pollutants enter the unsaturated zone through infiltration processes or industrial and municipal sewage leakage. Organic chemicals in the unsaturated zone move vertically throughout the groundwater table as they have a higher density (Mackay and Cherry, 1989; Fetter, 2001). The groundwater quality parameter is one of the critical parameters considered in groundwater as a raw water source for drinking water. Increasing groundwater use as a source of drinking water in Yogyakarta requires an in-depth study on groundwater quality, considering the high contribution of groundwater to raw water. In

Yogyakarta City, one of the causes of the deterioration in groundwater quality is pollution from household activities. Additionally, other factors, such as pollution from industrial, agricultural, other urban activities, also contribute significantly to changes in the groundwater environment (Putra, 2004; Hendrayana and Putra, 2019)

At the Yogyakarta City Railway Station, from 1997 to 1998, there was a leakage of 300 litres of diesel per day from diesel storage tanks for trains (Susilo, 2003; Setyaningsih, 2010; Wijaya, 2015; Hendrayana and Putra, 2019; Priambodo, 2020). That case was presumably due to a leak in the diesel storage tank. In 2001, the Yogyakarta City Railway Station community discovered diesel in the dug wells, which was thought to be caused by the leak. Based on the discovery of diesel in the dug wells, identifying the distribution of hydrocarbon contaminants in groundwater and zonation of polluted areas was carried out. Diesel is an organic chemical that belongs to the type of Light Nonaqueous Phase Liquid (LNAPL), which consists of a natural organic carbon chain, which can then be identified based on the level of Total Organic Carbon (TOC) (Newell et al., 1995; Schreier et al., 1999). The calculation of the TOC level is considered very fast and easy to measure the pure organic content in diesel. The TOC levels that indicate diesel in the unsaturated zone have a value of more than 30,000 ppm (Schreier et al., 1999; Tomlinson et al., 2014).

Based on the problems mentioned above, in restoring land contaminated with diesel, it is necessary to study the distribution of diesel contaminants in the unsaturated zone around the Yogyakarta City Train Station. This research aims to identify TOC levels in the unsaturated zone, Analyze the distribution of TOC levels in the unsaturated zone horizontally and vertically, and determine the location of diesel pollutant sources in the research area.

Materials and Methods

The study area is part of a depression known as the Yogyakarta Basin, formed by the uplifting processes of the Southern Mountains in the east and the Kulon Progo Mountains in the west about 1.6 million years ago. The Yogyakarta Basin is bounded by Mount Merapi in the north and the Indian Ocean in the south (Rahardjo et al., 1995). According to Husein and Srijono (2010), especially on the morphogenetic aspect, the research area is included in the volcanic landscape influenced by volcanic activity from the Tertiary to the present. The research area shows the Moderately Curvy Volcanic Foot with a flat to a moderately steep slope of 0 to >15% and a parallel drainage pattern. The river valley is widening to the south and is increasingly meandering. This research consisted of 3 stages, (1) preparation and literature study, (2) data collection, and (3) data analysis and report preparation. The preparation and literature study phase began with a literature review from previous related publications. After that, the tools and materials for this research were prepared. The data collection phase began with mapping surface lithology, identifying land use, mapping dug wells, measuring the groundwater table's depth, the elevation of the land surface, and taking soil samples in the research area. Soil samples were taken from 14 shallow core drilling in 2018 and 9 deep core drilling in 2019. The number of soil samples from shallow core drilling was 28 samples and 18 samples from deep core drilling. A lithological log from the ground surface to a depth of approximately 15 m accompanied each deep core drilling. Soil sample preparation was carried out using a standardized procedure before being analyzed in a laboratory.

The data analysis and report preparation phase began with measuring TOC levels in 46 soil samples. Data analysis was done using sample analysis results from the laboratory and direct measurements in the field. Analysis and evaluation of data were presented in the form of a zonation map of the distribution of TOC levels, a map of groundwater flow patterns, and a fence diagram for the distribution of the TOC horizontally and vertically. The analysis was carried out from the soils from shallow and deep core drilling. The data from these soils were used to show TOC levels from the soil surface and the subsurface. At a depth of 30 cm, the TOC levels in the soil ranged from 12,790 to 88,.270 ppm. The lowest TOC level was at the YP-14 point. Meanwhile, the highest TOC level was at the YP-10 point. At a depth of 50 cm from the soil surface, the TOC levels in the soil ranged from 17,500-90,870 ppm. The lowest TOC level was at point YP-14, while the highest TOC level was at point YP-1. The TOC levels for shallow core drilling samples can be seen in Table 1.

In general, the TOC levels at a depth of 50 cm were higher than the TOC levels at 30 cm. Only at points YP-2, YP-6, YP-11, YP12, and YP-15 were the TOC levels at a depth of 50 cm lower than the TOC levels at 30 cm. Drilling boreholes were carried out by deep core drilling with a depth of 15-17 m. Core samples from each drilled well were taken at two depth intervals for TOC levels in the laboratory. Soil/rock samples from the rock core were generally taken at shallow and medium depth intervals at intervals of 4 to 5 and 10 to 11 m. At shallow depth intervals (4-5 m), TOC levels in the soil ranged from 340 to 30,100 ppm. The point with the lowest TOC level was in the BM-4 well. Meanwhile, the drilled well with the highest TOC level was BM-2. At intermediate-depth intervals (10-11 m), TOC levels in the soil ranged from 380 to7,970 ppm. The point with the lowest TOC level was in the BM-4 well. Meanwhile, the drilled well with the highest TOC level was BM-2. The TOC levels of the deep core drilling sample are shown in Table 2.

Table 1. Laboratory test result for shallow core drilling.

Point Code	Depth (cm)	Coordinate		TOC Content (ppm)
		X	Y	
YP-1	30	429480	9139005	85,170
	50			90,870
YP-2	30	429453	9139007	34,900
	50			33,210
YP-3	30	429435	9139006	52,000
	50			58,790
YP-4	30	429521	9139004	40,110
	50			47,270
YP-5	30	429483	9139025	49,090
	50			56,010
YP-6	30	429406	9139005	37,100
	50			35,210
YP-7	30	429553	9138971	46,340
	50			58,140
YP-8	30	429517	9138982	62,900
	50			69,550
YP-9	30	429514	9138969	17,120
	50			18,680
YP-10	30	429495	9138972	88,270
	50			88,670
YP-11	30	429433	9138989	50,970
	50			49,010
YP-12	30	429458	9138987	77,550
	50			58,150
YP-13	30	429452	9138979	25,650
	50			30,540
YP-14	30	429411	9138991	12,790
	50			17,500

Table 2. Laboratory test result for deep core drilling.

Point Code	Depth (m)	Coordinate		TOC Content (ppm)
		X	Y	
BM-1	4-5	429648	9139009	1,860
	10-11			3,230
BM-2	4-5	429590	9139005	30,100
	10-11			7,970
BM-3	4-5	429542	9139012	1,350
	10-11			1,090
BM-4	4-5	429616	9138958	340
	10-11			380
BM-5	4-5	429571	9138972	1,180
	10-11			1,980
BM-6	4-5	429508	9138970	1,240
	10-11			1,640
BM-7	4-5	429465	9138978	7,260
	10-11			1,200
BM-8	4-5	429448	9139005	700
	10-11			1,080
BM-9	4-5	429405	9138993	1,250
	10-11			1,280

Geology and hydrogeology

The quaternary volcanic activity of Mount Merapi fills the Yogyakarta Basin unconformably above Tertiary rocks (MacDonald and Partners, 1984; Hendrayana, 1993; Hendrayana and Putra, 2004). Based on the regional geological map of the Yogyakarta Sheet (Surono et al., 1992; Rahardjo et al., 1995), the study area is part of the Young Merapi Sediment Formation. The Young Merapi Sediment Formation is divided into two formations, the Sleman Formation, which fills the lower part of the basin, and the Yogyakarta Formation, serving the upper part of the basin. In general, these two formations are composed of fluvial-volcanic deposits of gravel, sand, silt, and clay sizes (Hendrayana, 1993; Putra, 2004). Most Yogyakarta City has gravelly sand lithology in the south and medium to fine sand deposits in the north. In the study area, surface lithology covers fine sand to gravel (Djaeni, 1982; MacDonald and Partners, 1984; Iqbal, 2013).

The groundwater flow system in the study area is part of the Merapi Aquifer System. The Merapi Aquifer System in the Yogyakarta Graben, filled with river deposits and volcaniclastic deposits, is called the Yogyakarta-Sleman Groundwater Basin. Two main rivers border this basin, Opak River in the east and Progo River in the west (Hendrayana, 1993; Putra, 2004). Most research areas consist of an unconfined aquifer that is dominated by the intergranular flow. The groundwater system in the Yogyakarta City area is part of the unconfined aquifer with high productivity (Djaeni, 1982; Hendrayana, 1993).

A re-evaluation of borehole log data (Hendrayana and Putra, 2004) showed that the bedrock of the Merapi Aquifer System is composed of the Old Merapi Volcanic Deposits in the north Nglanggran and Semilir Formations in the east and the Sentolo Formation in the west and south. Hydraulic conductivity of the Merapi Aquifer System ranges from 0.8 m/sec to 95 m/sec with an average value of 8.6 m/sec. Storativity values range from 0.001 to 0.25. The difference in hydraulic pressure between the semi-confined aquifer at the bottom and the unconfined aquifer at the top causes groundwater to flow from the lower aquifer to the upper aquifer (Hendrayana, 1993; Hendrayana and Putra, 2004).

In general, the direction of groundwater flow in Yogyakarta City is north-south, with the Mount Merapi area as the groundwater recharge area and the southern area as the discharge area. In some areas, the direction of groundwater flow is not uniform, flowing to the west and east (Iqbal, 2013). The difference in the direction of groundwater flow is influenced by the presence of rivers that cut through Yogyakarta City, such as the Progo River, Opak River and Oyo River, and several other river branches. In the study area, the direction of groundwater flow is relatively west-east under the influence of Winongo River in the west and Code River in the east of the study area.

The groundwater availability in the study area was represented by groundwater in dug wells and groundwater seepage found around Winongo River. The groundwater level measurements in dug wells in 2019 were used to make a groundwater table map and groundwater flow pattern map in the study area. The research area has a varying groundwater table from 4 to 16 m from the ground surface. The groundwater table depth map was generated by plotting the groundwater table depth values for dug wells in 2019 using the IDW (Inverse Distance Weighting) interpolation method (Figure 1).

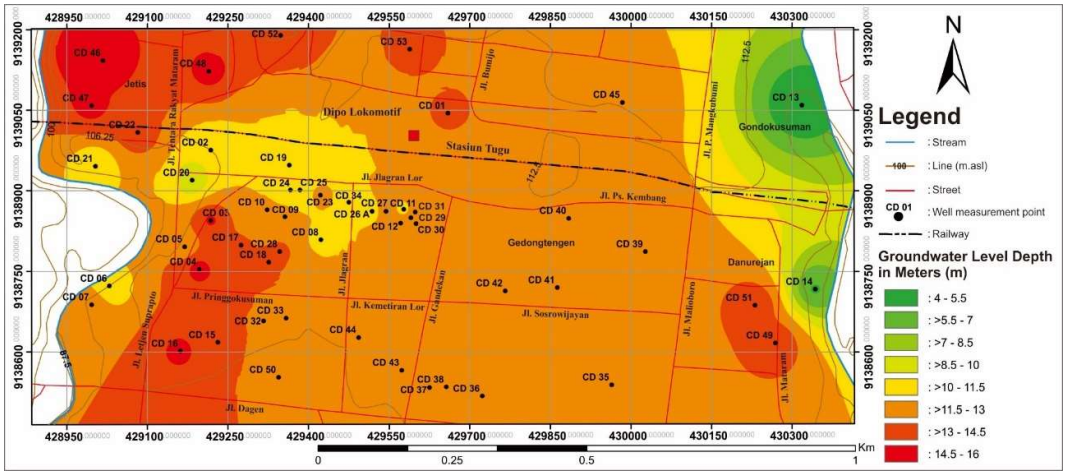

Figure 1. Map of groundwater level depth.

The groundwater table depth map shows the various depths of the groundwater table with a patchy pattern due to the influence of different elevations on the ground surface. The shallowest groundwater was found east of the study area around Code River, while groundwater around Winongo River was lower. The groundwater flow pattern map was reconstructed based on the groundwater table measurements in 53 wells. The research area had a groundwater table ranging from 94 to 102 m above sea level (asl). The highest groundwater level is in the north of the study area, with lower elevations in the east, west, and south. Groundwater in the study area flows to the west, east, and south (Figure 2).

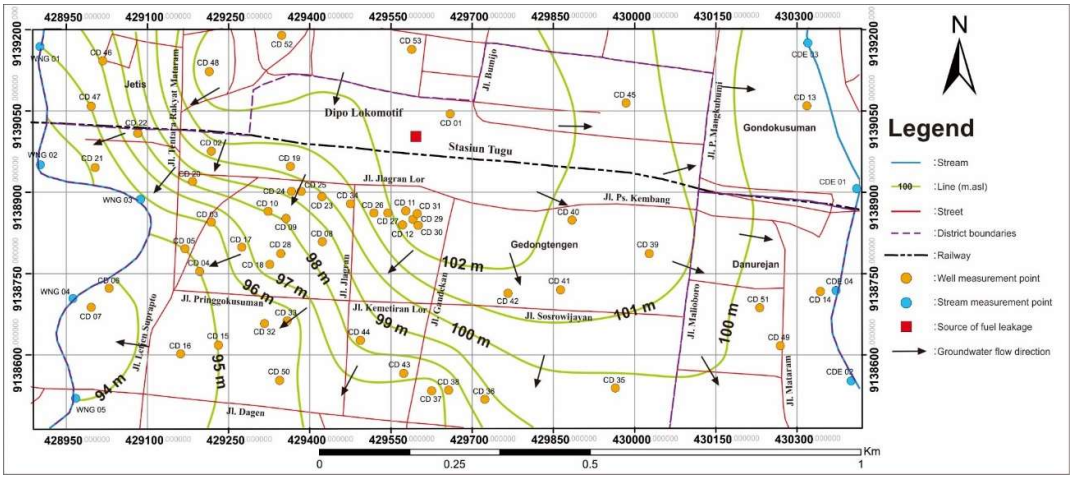

Figure 2. Map of groundwater flow pattern.

The Winongo River controls the west and east groundwater flows in the west, and the Code River controls the groundwater flow in the east. These two rivers are gaining streams, where the rivers get their supply from groundwater due to the higher groundwater level than the river water level. The shallow core drilling and deep core drilling data from October to December 2019 were used for subsurface stratigraphic analysis. The shallow core drilling data was born at 14 points, and deep core drilling was

carried at 9 points. The coordinates of the shallow and deep core drilling locations are shown in Tables 3 and 4. The distribution of the surface rock is obtained from the correlation of drill log data. The lithology in the research area is divided into four groups, namely filled soil, sand, alternating sand-clayey sand- sandy clay, and clay. Shallow and deep core drilling sampling locations are shown in Figure 3.

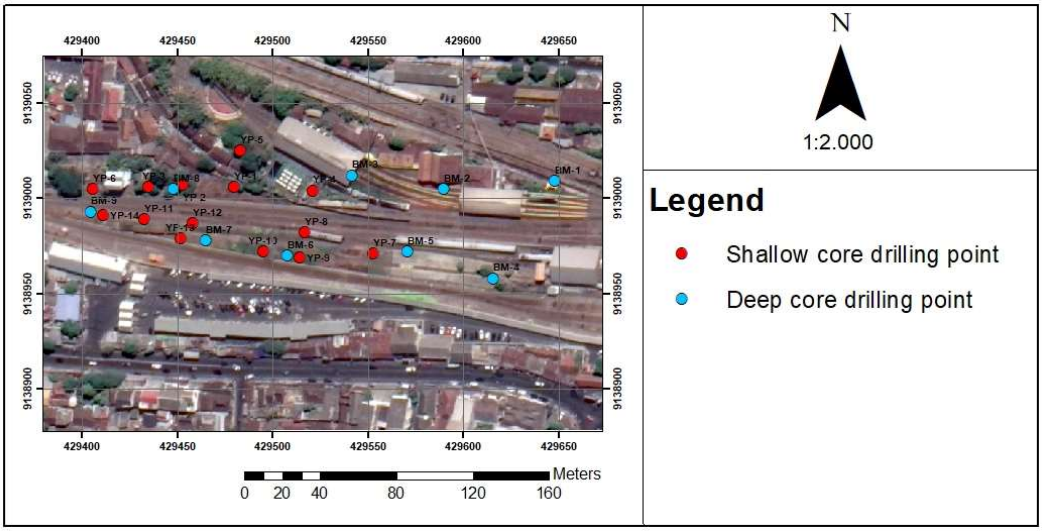

Figure 3. The location of shallow and deep core drilling.

Table 3. Shallow core drilling data.

Point Code	Coordinate		Drilling Depth (cm)	Lithology
	X	Y		
YP-1	429480	9139005	30	
			50	
YP-2	429453	9139007	30	
			50	
YP-3	429435	9139006	30	
			50	
YP-4	429521	9139004	30	
			50	
YP-5	429483	9139025	30	
			50	
YP-6	429406	9139005	30	
			50	
YP-7	429553	9138971	30	
			50	
YP-8	429517	9138982	30	Soil
			50	
YP-9	429514	9138969	30	
			50	
YP-10	429495	9138972	30	
			50	
YP-11	429433	9138989	30	
			50	
YP-12	429458	9138987	30	
			50	
YP-13	429452	9138979	30	
			50	
YP-14	429411	9138991	30	
			50	

Table 4. Deep core drilling data.

Point Code	Coordinate X	Coordinate Y	Drilling Depth	Lithology
BM-1	429648	9139009	15 m	top soil (0-2 m), interlude of sand-sandy clay-clay sand (2-4 m; 4.5-8.5 m), sand (4-4.5 m; 8.5-14.5 m), clay (14.5-15 m)
BM-2	429590	9139005	15 m	top soil (0-2 m), sand (2-5.5 m; 10-14.5 m), interlude of sand-sandy clay-clay sand (5.5-10 m)
BM-3	429542	9139012	15 m	top soil (0-2 m), sand (2-10.5 m), interlude of sand-sandy clay-clay sand (10.5-15 m)
BM-4	429616	9138958	15 m	soil (0-2 m), interlude of sand-sandy clay-clay sand (2-8 m), sand (8-11.5 m; 13-15 m), clay (11.5-13 m)
BM-5	429571	9138972	17 m	top soil (0-2 m), interlude of sand-sandy clay-clay sand (2-10 m), sand (10-11.5 m; 12-17 m), clay (11.5-12 m)
BM-6	429508	9138970	17 m	topsoil (0-2 m), interlude of sand-sandy clay-clay sand (2-8.5m), sand (8.5-17 m)
BM-7	429465	9138978	17 m	top soil (0-2 m), sand (2-10 m; 16-17 m), interlude of sand-sandy clay-clay sand (10-16 m)
BM-8	429448	9139005	17 m	top soil (0-2 m), sand (2-17 m)
BM-9	429405	9138993	17 m	top soil (0-2 m), sand (2-12 m; 14-17 m), interlude of sand-sandy clay-clay sand (12-14 m)

The surface lithology is filled soil. Then beneath the filled soil, there are three types of lithology: (1) brown sand deposits, fine-very coarse (0.125-2 mm) sand, characterized as naturally loose, highly porous, and in a composition of fine-very coarse sand material. (2) interlude sand-clayey sand-sandy clay consisting of several lithologies, namely sand deposits, clayey sand deposits, and sandy clay deposits.

Clayey sand deposits are blackish-brown in colour, with a grain size of clay to medium sand (1/256-0.5 mm), loose, medium to high porosity, and with the composition of clay and medium-sized sand, which is more dominant. Sandy clay deposits are brownies black in colour, with grain size of clay to medium sand (1/256-0.5 mm), loose, medium to high porosity, and the composition is predominantly clay and medium-sized sand. (3) Clay lithology is a thin minor deposit and is in the form of tiny lenses. The Black clay deposits with grain size (<1/256 mm), loose, low porosity have clay material composition. The lithology log fence diagram of the study area can be seen in Figure 4.

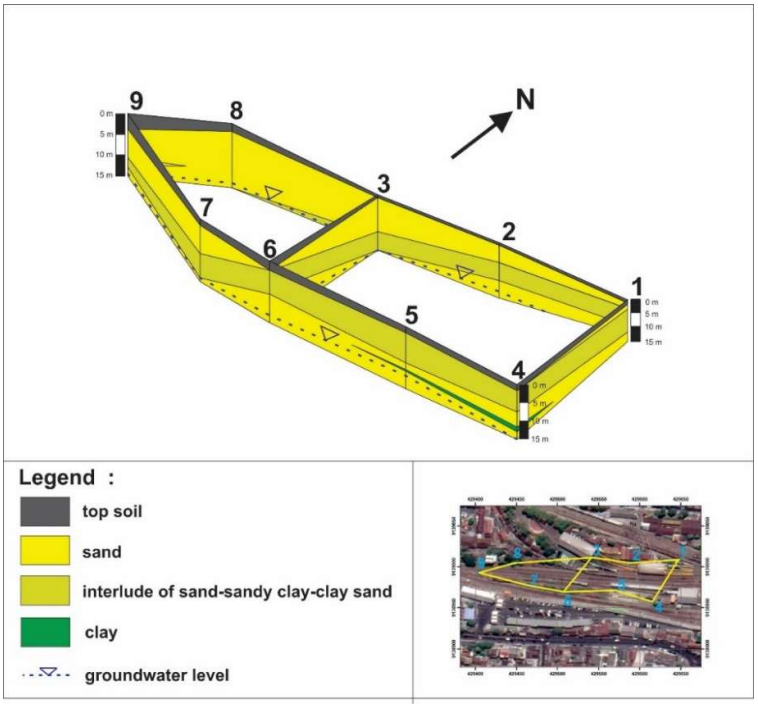

Figure 4. Lithology fence diagram.

Results and Discussion

The TOC content map was constructed based on the total TOC levels at all points of each depth. Each point in the shallow and deep core drilling had two levels of TOC, of a depth of 30 cm and 50 cm, and the depth of 5 m and 10 m. Based on the TOC levels obtained, a zonation map was made at each depth. TOC levels consist of 6 classes: green (0-6,000 ppm), yellowish-green (6,000-12,000 ppm), yellow (12,000-18,000 ppm), orange (18,000-24,000), reddish-orange (24,000-30,000 ppm), and red (>30,000 ppm). The zonation map used two interpolation methods, the Inverse Distance Weighted (IDW) method and Kriging using two software: ArcGIS and Surfer.

TOC level map at a depth of 30 cm using the IDW method showed the appearances of 5 colour classes, with the dominance of red (>30,000 ppm). The TOC content map at a depth of 30 cm using the Kriging method showed only one colour, red (>30,000 ppm). The results of the interpolation of the two ways were almost the same. The TOC level in this area was highest at STA 10, with 88,270 ppm, while the lowest was in the southern part of STA 14, with 12,790 ppm. The TOC content map at a depth of 30 cm is shown in Figure 5. From the TOC content map with a depth of 50 cm using the IDW method, the formed zones were almost the same as the zones in the TOC level map at a depth of 30 cm. It was also found that the red zone was dominant (>30,000 ppm) among four color classes. The map for TOC levels at a depth of 50 cm using the Kriging method also showed the overall zone was only red (>30,000 ppm). There was an increase in TOC level on YP-7 from a depth of 30 cm to 50 cm. The TOC level in this area was highest at YP-1, with 90.870 ppm, while the lowest level was in the southern part, at YP-14, with 17,500 ppm. There was a TOC level that increased from a depth of 30 cm to 50 cm. The map of TOC levels at a depth of 50 cm can be seen in Figure 6.

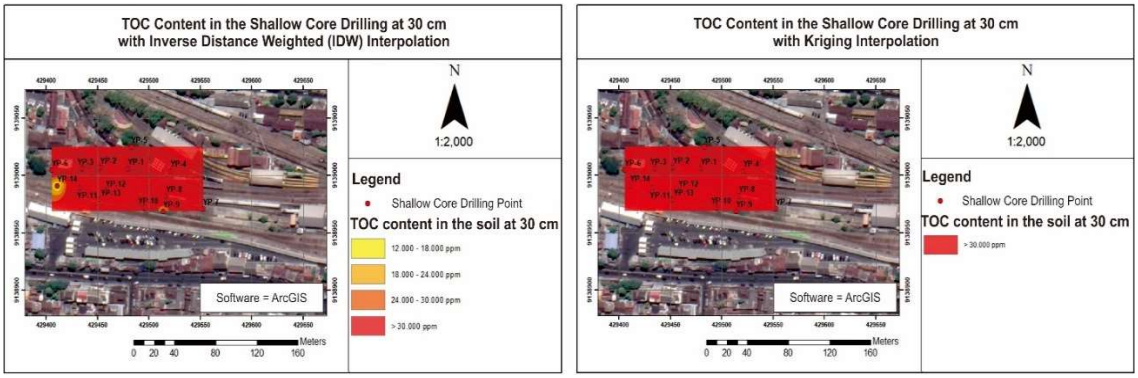

Figure 5. Map distribution of TOC levels at 30 cm shallow core drilling with inverse distance weighted (left) and Kriging method (right).

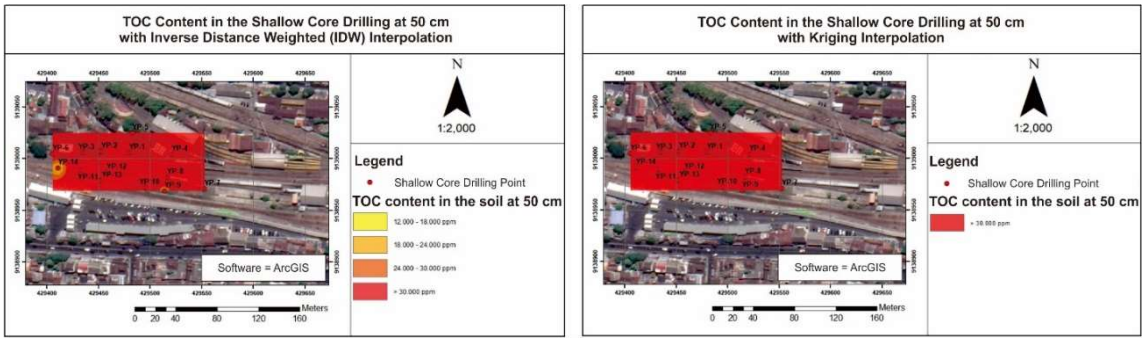

Figure 6. Map distribution of TOC levels at 50 cm shallow core drilling with inverse distance weighted (left) and Kriging method (right)

The map of TOC levels at a depth of 4-5 m using the IDW method shows that there was a red zone (>30,000 ppm) at BM-2 and a decrease in TOC levels to reddish-orange (24,000-30,000 ppm) and green (0-6,000 ppm). The TOC level in this area was highest at BM-2, with 30,100 ppm, while the lowest was in the western part, at BM-1, with 1,860 ppm. TOC level map of a depth of 4-5 m using the Kriging method shows that the predominant zone was green, with a small area of yellowish-green. In the results of the Kriging method,

there was no visible difference at point BM-2. There was a decreasing level of TOC from a depth of 50 cm to 5 m. The map of TOC levels of a depth of 5 m can be seen in Figure 7. The map of TOC levels of a depth of 10-11 m using the IDW method shows the dominance of the green zone (0-6,000 ppm). The TOC level at BM-2 is the highest, with 7.370 ppm, while the lowest was in the southeastern part, at BM-4, with 380 ppm. The TOC level map for a depth of 10-11 m using the Kriging method shows that the formed zonation was almost identical to the zonation using the IDW method. The difference between the two methods was the width of a yellowish-green zone (6,000-12,000 ppm). There was a decreasing level of TOC from a depth of 5 m to 10 m. The map of TOC levels of a depth of 10 m can be seen in Figure 8.

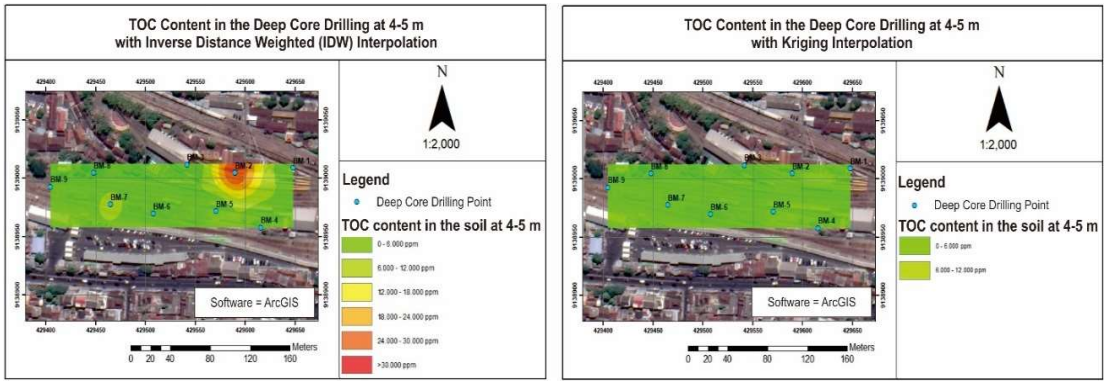

Figure 7. Map distribution of TOC levels in 4-5 m deep core drilling with inverse distance weighted (left) and Kriging method (right).

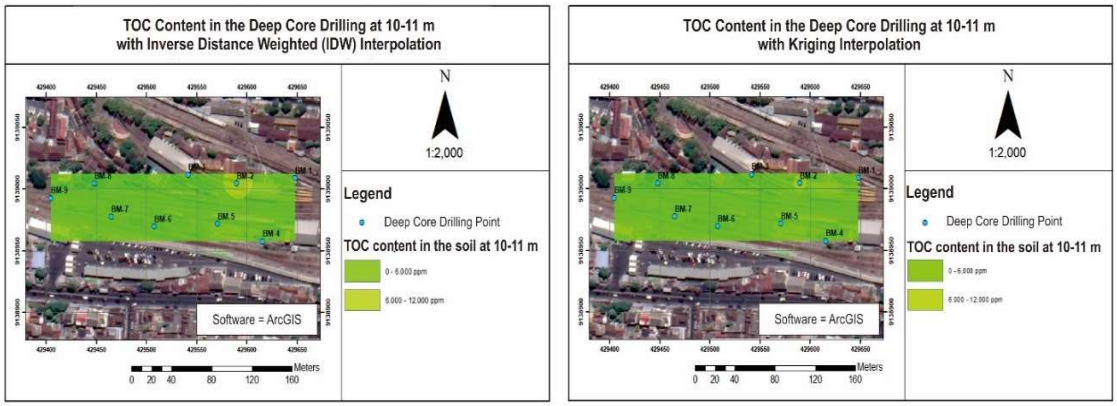

Figure 8. Map distribution of TOC levels in 10-11 m deep core drilling with inverse distance weighted (left) and Kriging method (right).

\

The TOC level map of 30 cm using the IDW method run with Surfer shows that the zone consisted of 5 colour classes dominated by red (>30,000 ppm). In the TOC content map of a depth of 30 cm using the Kriging method, the overall zone was red (>30,000 ppm) and consisted of 5 classes. The interpolation results of the two ways were almost the same, but there was a widening zone in the west. The TOC level in this area was highest at STA 10, with 88,270 ppm, while the lowest was in the southern part, at STA 14, with 12,790 ppm. The TOC content map of a depth of 30 cm is displayed in Figure 9. The TOC level map of a depth of 50 cm using the IDW method run with Surfer shows that the zone was almost the same as the zone in the TOC level map of 30 cm – 4 colour classes with predominantly red (>30,000 ppm). The TOC level map of a depth of 50 cm using the Kriging method also shows four colour classes with mostly red (>30,000 ppm). There was an increase in TOC level at YP-7 from a depth of 30 cm to 50 cm. The TOC level in this area was 90,870 ppm at YP-1, while the lowest was in the southern part of YP-14, with 17,500 ppm. There was an increasing TOC level from a depth of 30 cm to 50 cm. The map of TOC levels of a depth of 50 cm is shown in Figure 10. The map of TOC levels of a depth of 4-5 m using IDW run with Surfer showed a red

(>30,000 ppm) zone at BM-2 and a decreasing TOC level to reddish-orange (24,000-30,000 ppm) and green (0-6,000 ppm). Meanwhile, the TOC level map of a depth of 4-5 m using the Kriging method shows results that were almost the same as the results of the IDW method, and there was only a difference in the width of the red zone (>30,000 ppm). The TOC level in this area was highest at BM-2, with 30,100 ppm, while the lowest was in the western part, at BM-1, with 1,860 ppm. There was a decreasing level of TOC from a depth of 50 cm to 5 m. The map of TOC levels of a depth of 5 m is shown in Figure 11.

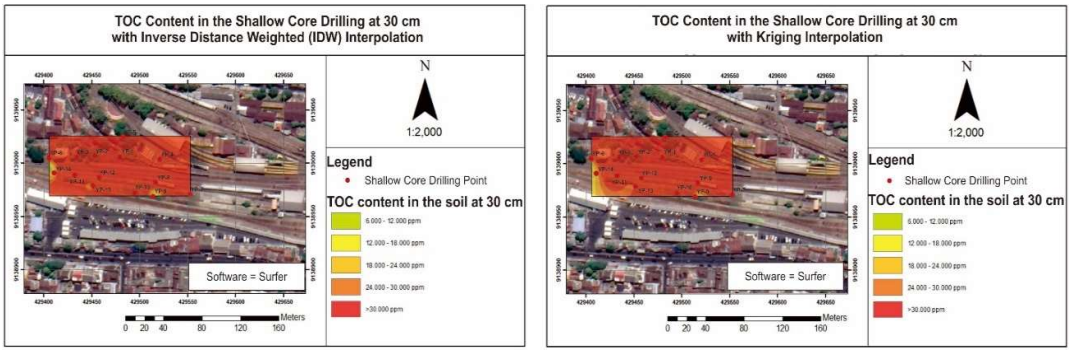

Figure 9. Map distribution of TOC levels in 30 cm shallow core drilling with inverse distance weighted (left) and Kriging method (right).

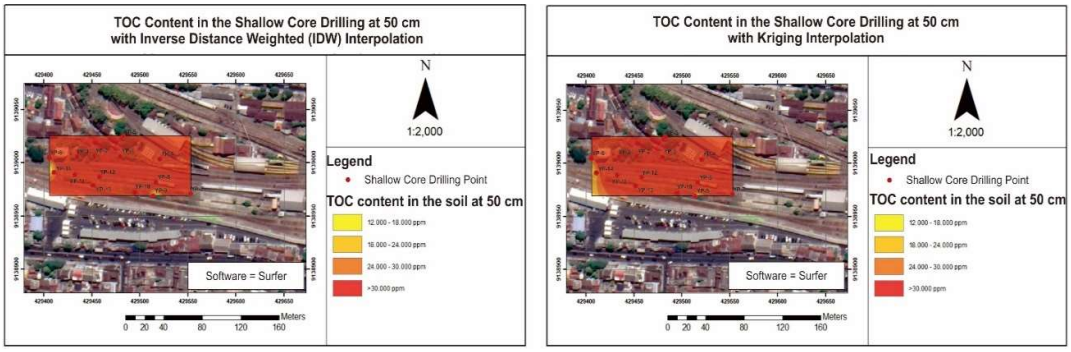

Figure 10. Map distribution of TOC Levels in 50 cm shallow core drilling with inverse distance weighted (left) and Kriging method (right).

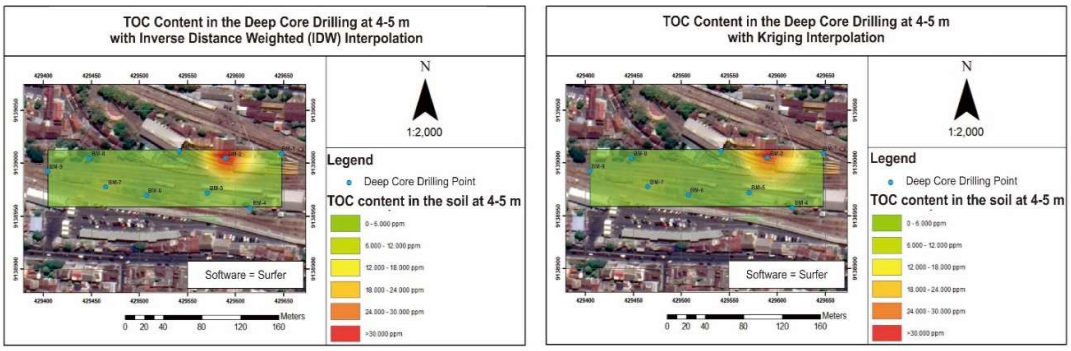

Figure 11. Map distribution of TOC levels in 4-5 m deep core drilling with inverse distance weighted (left) and Kriging method (right).

The TOC level map of a depth of 10-11 m using the IDW method run with Surfer shows two colour classes with the dominance of the green zone (0-6,000 ppm). The TOC level map of a depth of 10-11 m using the Kriging method showed that the resulted zones were almost the same as the zones of the IDW method. The difference in the results of the two ways was in the area of the yellowish-green zone (6,000-12,000 ppm). The highest level of TOC was at BM-2, with 7,370 ppm, while the lowest was in the southeastern part, at BM-

4, with 380 ppm. There was a decreasing level of TOC from a depth of 5 m to 10 m. The map of TOC levels of a depth of 10 m is shown in Figure 12. Primary stratigraphic data from the lithology log was used to determine 2D and 3D subsurface conditions. Each shallow and deep core drilling data had a different TOC level. The BM-2 lithology log showed lithological log data with a graph of TOC levels and a soil physical property in the form of odour. The location of the BM-2 was near a site that was thought to be the source of the pollution. The TOC level graph showed an anomaly with increasing TOC levels at a depth of 4-5 m and 10-11 m. This anomaly was indicated the presence of diesel contaminants in the soil. The availability of diesel contaminants in the soil is reinforced by the odour that exists at these depths. The peak of TOC level as shown in the TOC graph, especially at a depth of 4-5 m, indicated that there was a possibility that the location around the BM-2 drilling point was the location of the pollutant source.

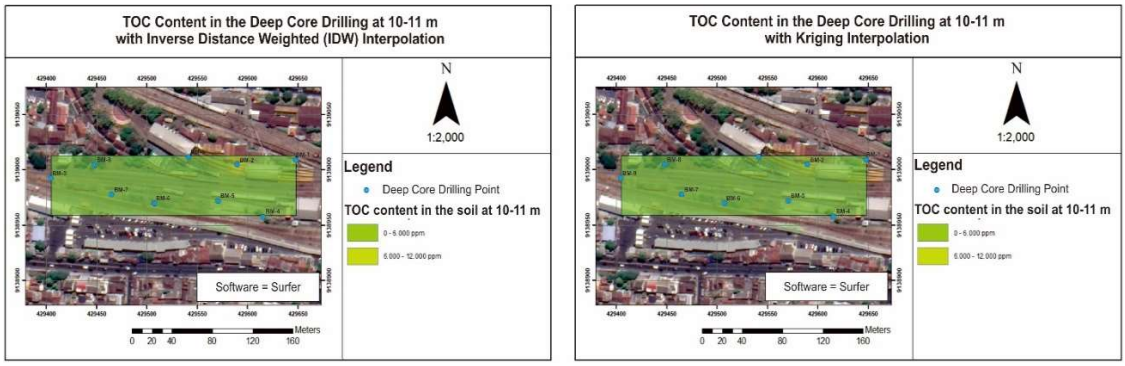

Figure 12. Map distribution of TOC levels in 10-11 m deep core drilling with inverse distance weighted (left) and Kriging method (right).

The lithology log of BM-5 is located in the southern part of BM-2. The TOC graph did not show any anomalies as indicated by the increase in TOC level at a depth of 4-5 m and 10-11 m, but it had a physical characteristic in the form of a diesel odor starting from a depth of 10 m downwards. There was also no TOC level peak shown in the TOC level graph. The lithology log showed high TOC levels and the smell of diesel on sand lithology at a depth of 10-15 m. The high TOC levels were because the dominant lithology at this depth was sand. Smaller lithological sand grain sizes such as loamy sand, sandy loam, and clay at a depth of 10-15 m also had a diesel odour. The clay had a more potent smell because the material is fine grain size and can absorb pollutants better than the larger grain sizes.

In general, the unsaturated zone in the study area was at a depth of 30 and 50 cm below the soil surface and showed a very high TOC level. A reasonably high TOC level was found at a depth of 4-5 m, and a depth of 10-11 m had a relatively lower TOC level. The TOC level, which was relatively high at BM-2 at a depth of 4-5 m, can be interpreted as that this location was the source of diesel contaminants. In other drilled logs at a depth of 4-5 m had low TOC levels. The correlation of the TOC levels with the stratigraphy of the study area in detail can be seen in Figure 13. In the distribution map of TOC levels using the Inverse Distance Weighted (IDW) and Kriging methods, an interpolation method that is suitable and able to describe the current condition of the research area was determined. The map also compared the interpolation results from 2 software, ArcGIS and Surfer. Qualitatively, the interpolation results from ArcGIS and Surfer had differences on the TOC level map for deep core drilling at a depth of 4-5 m, especially in the interpolation results of the Kriging method. The interpolation results of the Kriging method on ArcGIS showed the dominant green colour (0-6,000 ppm), while Surfer's results were almost the same as the results using the IDW method, so the Kriging method on ArcGIS cannot be used in this case. The map of the distribution of TOC levels in the deep core drilling soil at a depth of 4-5 m shows the condition where the location of BM-2 was the location of the diesel pollutant source. The map also shows the existence of zones with a decreasing TOC level. The IDW interpolation method considers the distance and value of the surrounding points so that the IDW method describes the actual conditions. In contrast, the Kriging interpolation method considers all existing points. The result related to Bhunia et al. (2018) IDW is the best method for TOC modelling. The fence diagram shows high TOC levels at a depth of 30 and 50 cm with values above 30,000 ppm. The high TOC levels can be interpreted as diesel waste because the area is a Locomotive Depot. The result related to Schreier et al. (1999) and Tomlinson et al. (2014) diesel in the unsaturated zone has a value of more than 30,000 ppm. Locomotives are repaired and cleaned in this location so that this location becomes a dispersion place of diesel waste on the ground.

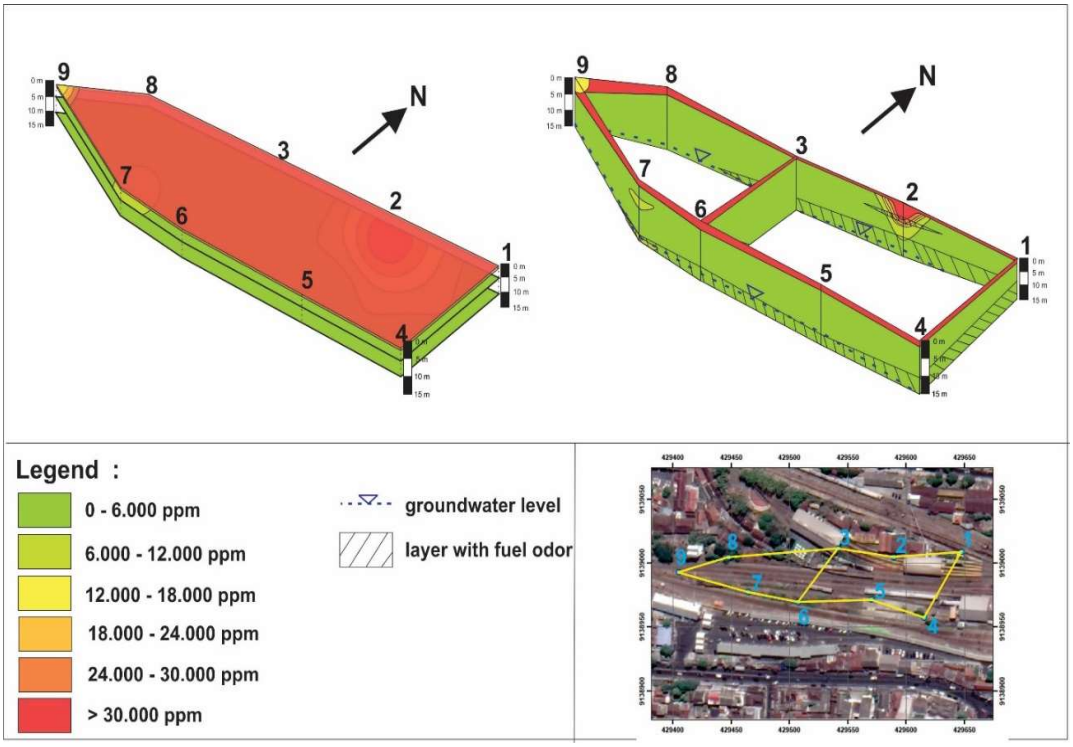

Figure 13. Fence diagram and horizontal slicing of TOC content.

The diesel waste is spread on the ground surface by surface water, which then infiltrates below the surface through the unsaturated zone and accumulates at a depth of 30 to 50 cm. The result related to Bedient et al. (1999) and Fetter (2001) the contaminants will break up into individual blobs and change from the free LNAPL phase to the residual LNAPL phase.

The fence diagram of TOC levels at the BM-2 location shows the zones of TOC levels from red to green from top to bottom. This colour indicates that the pollutant source at the point of BM-2 is below the surface, which is a place for storing diesel. Diesel waste at this location then flows downwards because diesel includes in the LNAPL type. Diesel waste that flows downwards is trapped in the soils to become a new source of pollution in a reasonably long time. The result related to Tomlinson et al. (2014) the pollutant can quickly spread away from its source. From the location of the BM-2 point, which is the location of the primary source of pollution, there is no significant distribution of TOC values to other sites because the distance of one another point locations is quite far. The process in BM-2 starts from the presence of diesel waste deposited at a depth of 5 m. Through the percolation process, the diesel waste flows upward until it reaches the groundwater level at a depth of 14 m. This diesel waste is deposited above the groundwater table because its density is smaller than the density of water. There is a seasonal change in groundwater level in the rainy season and dry season, so some of the diesel waste will be left behind in the soil layer in the unsaturated zone in the third phase of LNAPL water-LNAPL-air residue.

Figure 14 shows that there are areas with the smell of diesel and regions without diesel odour. The smell of the diesel area is close to the source of the diesel pollutant. The site without the smell of diesel is far from the source of the diesel pollutant. The flow of groundwater influences the movement of diesel contaminants indicated by red arrows. Diesel pollutants will follow the direction of groundwater flow to the south so that the movement of diesel pollutants also heads to the south (Setyaningsih, 2010; Wijaya, 2015). A boundary line between the area with the smell of diesel and the site without diesel smell is the basis for interpreting the furthest limit for groundwater flow in the study area. The flow of diesel pollution to the east is indicated by a thick layer of diesel smells at BM-1 and BM-4, which is the easternmost boundary of the study area. If the lithology log fence diagram and the TOC level fence diagram are combined, it shows that the sand lithology at the top and bottom has a different smell of diesel. Alternating layers of sand-clayey sand-sandy clay limit the upper and lower sand lithology. The contaminated diesel pollutants aquifer located on the lower sand lithology where groundwater level fluctuations occurred.

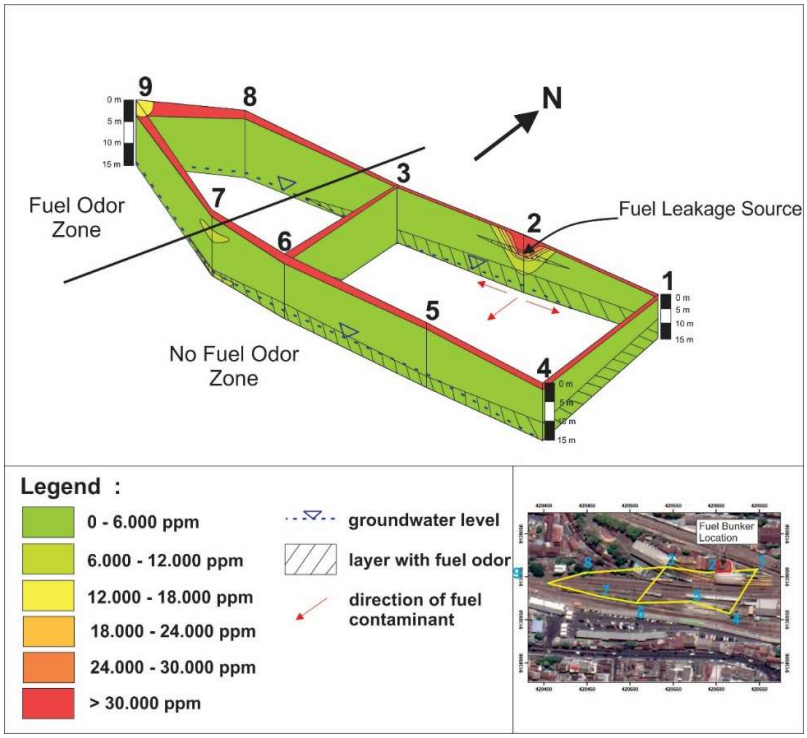

Figure 14. The direction of LNAPL movement**.**

Conclusion

Soils in the unsaturated zone are proven to be polluted by diesel. The analysis of TOC levels in shallow core drilling ranged from 12,790-90,870 ppm, and deep core drilling ranged from 340-30,100 ppm. The distribution of diesel pollution in the vertical direction shows a lower TOC value but still indicates the smell of diesel. The diesel pollution source is in the location of the former diesel tank at the Yogyakarta Railway Station Locomotive Depot. At the location of this pollutant source, there is a vertical movement of diesel pollutants to a depth of 10-15 m following fluctuations in the groundwater level accordingly and spreads following groundwater flow.

Acknowledgements

The authors would like to thank all parties who have supported the preparation of this paper, especially the Department of Geological Engineering, Faculty of Engineering, Gadjah Mada University, and PT. Indonesian Railways DAOP 6 Yogyakarta.

References

Bedient, P.B., Rifai, H.S. and Newell, C.J. 1999. *Groundwater Contamination: Transport and Remediation.* 2nd edition. Prentice-Hall, USA, 624 p.

Bhunia, G.S., Shit, P.K. and Maiti, R. 2018. Comparison of GIS-based Interpolation Methods for Spatial Distribution of Soil Organic Carbon (SOC). *Journal of The Saudi Society of Agriculture Science* 17:114-126, doi:10.1016j.jssas.2016.02.001.

Djaeni, A. 1982. Hydrogeological Map of Indonesia Scale 1:250.000 *Sheet IX Yogyakarta*. Directorate of Environmental Geology, Bandung (*in Indonesian*).

Fetter, C.W. 2001. *Applied Hydrogeology.* 4th edition. United States, Prentice-Hall.

Hendrayana, H. 1993. Hydrogeologie und Groundwassergewinnung Im Yogyakarta Becken, Indonesien. Dissertation, RWTH-Aachen.

Hendrayana, H. and Putra, D.P.E. 2004. The Improvement of Yogyakarta Groundwater Basin Concept. Department of Geological Engineering, Gadjah Mada University, pp. 1–9 (*in Indonesian*).

Hendrayana, H. and Putra, D.P.E. 2019 Survey Report and Measurement of Groundwater Pollution Parameters at Tugu Station, Yogyakarta. LKFT Study Center, Faculty of Engineering, Gadjah Mada University, Yogyakarta (*in Indonesian*).

Husein, S. and Srijono. 2010. Geomorphological Map of Yogyakarta Special Province. Symposium of Geology, pp. 1-11 (*in Indonesian*).

Iqbal, M. 2013. Groundwater Flow Modeling in Yogyakarta City Area. Department of Geological Engineering, Faculty of Engineering, Gadjah Mada University (*in Indonesian*).

MacDonald and Partners. 1984. Greater Yogyakarta Groundwater Resources Study, Volume 3: Groundwater. Directorate General of Water Resources Development Project (P2AT), Ministry of Public Works, Government of The Republic Indonesia.

Mackay, D.M and Cherry, J.A. 1989. Groundwater contamination: pump and treat remediation. *Environmental Science and Technology* 23(6):630-636,

doi:10.1021/es00064a001.

Newell, C.J., Acree, S.D., Ross, R.R. and Huling, S.G. 1995. Ground Water Issue - Light Nonaqueous Phase Liquid. Environment Protection Agency (EPA), US, pp. 1-28.

Priambodo, Y. 2020. Total Organic Carbon (TOC) in the Unsaturated Zone at Pringgokusuman, Gedongtengen Regency, Yogyakarta. Department of Geological Engineering, Faculty of Engineering, Gadjah Mada University (*in Indonesian*).

Putra, D.P.E. 2004. Integrated water resources management in Merapi Yogyakarta Basin. *Warta Penelitian Universitas Gadjah Mada Special Edition* 5:44–49.

Rahardjo, W., Sukandarrumidi, and Rosidi, H.M.D. 1995. Geology Map of Yogyakarta, Java Sheet. Bandung: Geological Research and Development Center (*in Indonesian*).

Schreier, C.G., Walker, W.J., Burns, J. and Wilkenfeld, R. 1999. Total organic carbon as a screening method for petroleum hydrocarbons. *Chemosphere,* 39(3):503-510.

Setyaningsih, W. 2010. Movement model of diesel pollutants in sandstone aquifers of the young Merapi volcanic formation. *Journal of Geography* 7(2):75-87 (*in Indonesian*).

Surono, Toha, B. and Sudarno, I., 1992. Geological Map of Surakarta-Giritontro, Java. Bandung: Geological Research and Development Center (*in Indonesian*)..

Susilo, W. 2003. Solar Waste from Tugu Station Contaminates Residents' Wells. Retrieved From https://www.liputan6.com/news/read/51513/limbah-solar-stasiun-tugu-mencemari-sumur-warga, published on 19 March 2003.

Tomlinson, D.W., Thornton, S.W., Thomas, A.O., Leharne, S.A. and Wealthall, G.P. 2014. An illustrated handbook of LNAPL transport and fate in the subsurface, Contaminated Land: London, http://www.claire.co.uk/LNAPL.

Wijaya, S.Y.C. 2015. Groundwater Pollution from Diesel in Jlagran Village, Gedongtengen District, Yogyakarta City. Department of Geological Engineering, Faculty of Engineering, Gadjah Mada University, Yogyakarta (*in Indonesian*).